Validation of Parametric Roll Motion Predictions for a Modern Containership Design

Jörg Brunswig, *Germanischer Lloyd*

Ricardo Pereira, *Germanischer Lloyd*

Daewoong, Kim, *Daewoo Shipbuilding & Marine Engineering Co., Ltd.*

ABSTRACT

This paper describes recent efforts to validate two nonlinear time domain programs for simulation of ship motions. The results of the methods ROLLSS and GL SIMBEL were compared with model test measurements of a modern post-Panmax containership model carried out at Hamburg Ship Model Basin (HSVA). This model was designed by Daewoo Shipbuilding & Marine Engineering Co., Ltd. (DSME). Furthermore, to obtain reliable roll damping coefficients, roll damping tests were performed prior to the calculations. For different load cases the occurrence of parametric roll in regular waves was investigated for a range of speeds, wave lengths and wave heights. The computed and measured roll motions revealed a significant nonlinear behaviour with respect to wave height.

Keywords: *Parametric Roll, Simulation, Roll Damping, Validation*

1. INTRODUCTION

The results of an internal research project DYNAS - Dynamic Stability - carried out at Germanischer Lloyd (GL) since 2003 are presented. The first phase of this project just finished. A systematic application of the nonlinear sea keeping methods GL SIMBEL (Pereira, 2003) and ROLLSS (Petey, 1988) to predict the motion behaviour of modern Panmax-, Post-Panmax containerships in severe sea ways was performed. The focus of the first phase was to validate the methods ROLLSS and GL SIMBEL with emphasis on parametric roll. The second phase of DYNAS aims to establish GL classification rules to avoid parametric roll, pure loss of stability, and broaching-to phenomena.

2. PARAMETRIC ROLL

Large modern containerships are susceptible to what is known as parametric rolling (SNAME 2003). Dangerous parametric roll motions with large amplitudes in waves are induced by the variation of transverse stability between the position on the wave crest and the position in the wave trough. Parametric roll primarily occurs under the following conditions:
- Slender hull
- The primary wave system's wavelength varies between half and twice the ship's length
- The wave height exceeds a threshold level
- Almost ahead or astern wave heading
- Low roll damping
- The natural roll frequency ω_r of the ship is about half the encounter frequency ω_e or almost equal to the encounter

frequency.

For frequency ratios of $\frac{\omega_r}{\omega_e} = \frac{1}{2}$ in head waves or following waves, the stability varies with the encounter frequency ω_e which is approximately twice the roll frequency ω_r of the ship. The stability attains a minimum and maximum twice during each roll motion. The ship reaches the maximum roll angle in the wave trough, where the up-righting moment is large due to the increased stability. On the wave crest with low stability, the roll motion crosses zero. During one encounter period the ship gains energy twice and shows large amplitudes of symmetric rolling.

For frequency ratios of 1:1 in following waves, the stability attains a minimum and a maximum once during each roll motion. This situation is characterised by asymmetric rolling, i.e. the amplitude with the wave crest amidships is greater than the amplitude on the opposite side. In higher waves, parametric roll tends to occur within a bandwidth of frequency ratios between 0.9 and 1.1, see Figure 7.

3. SIMULATION METHODS

Because of two restrictions, linear sea keeping methods like GL PANEL (Papanikolaou/Schellin, 1991) or GL STRIP (Hachmann, 1991) are not suited to predict parametric roll. They do not account for stability changes caused by a passing wave, because the pressure forces are only integrated up to the undisturbed water surface. In addition, these methods are restricted to small amplitude ship motions. Therefore, they are incapable of predicting highly nonlinear phenomena such as parametric roll, which often leads to large roll angles.

The methods to be validated here remedy these problems by simulating in the time domain and treating the motions nonlinearly. We approach parametric roll investigations by the following two-step process:

ROLLSS (2 nonlinear degrees of freedom - surge and roll, very fast) is used to perform a large number of simulations to quickly identify regions of parametric roll occurrence.

GL SIMBEL (6 nonlinear degrees of freedom, slower) is used to yield more accurate results in these regions of interest.

3.1 ROLLSS

The method was first established by Söding (1982) and further developed by Kröger (1986) and Petey (1988). This time domain method uses response amplitude operators (RAO) computed with GL STRIP to determine the sway, heave, pitch, and yaw motions and simulates the surge and roll motions nonlinearly. The righting lever arm is calculated at each time step, using the concept of the equivalent wave (Söding 1982). The wave elevation at location x and time t is calculated by a superposition of all wave components in the chosen seaway spectrum:

$$\zeta(x,t) = \sum_{n=1}^{n_\omega} \Re\left[\hat{\zeta}_n \cdot e^{i(\omega_n t - k_n x \cos \mu_n)} \right] \quad (1)$$

where ω_n is the wave frequency, k_n the wave number and μ_n the wave direction. The equivalent wave is given by

$$\zeta(x,t) = \sum_{n=1}^{n_\omega} \Re\left[\hat{\zeta}_n \cdot e^{i(\omega_n t - k_n x \cos \mu_n)} \right] \quad (1)$$

$$\zeta_e(x,t) = \sum_{n=1}^{n_\omega} \Re\left[\left(\hat{a}_n + \hat{b}_n x + \hat{c}_n \cos \frac{2\pi x}{\lambda} \right) e^{i\omega_n t} \right] \quad (2)$$

where the coefficients $\hat{a}_n$, $\hat{b}_n$ and $\hat{c}_n$ are determined using the following minimisation problem:

$$\int_{-\frac{L}{2}}^{\frac{L}{2}} (\zeta(x,t) - \zeta_e(x,t))^2 dx = min! \qquad (3)$$

The wavelength of the equivalent wave is $\lambda = L_{pp}$, which is expected to yield the largest parametric roll excitation. The roll equation reads:

$$\ddot{\varphi} = \frac{M - d_L \dot{\varphi} - d_Q \dot{\varphi}|\dot{\varphi}| - (g-\ddot{z})mh(\varphi,T,\vartheta,t) - \ddot{\vartheta}\Theta_{xz} \sin\varphi}{\Theta_{xx}} \qquad (4)$$

where M is the wave excitation moment obtained from GL STRIP, and d_L and d_Q are linear and quadratic damping coefficients, respectively. Gravity and ship mass are denoted by g and m, and $\ddot{z}$ and $\ddot{\vartheta}$ are the heave and pitch accelerations calculated with GL STRIP. The righting lever arm h was pre-calculated as a function of roll angle φ, draught T and pitch angle ϑ using a hydrostatic method (user-coded NAPA Macros).

3.2   GL SIMBEL

The development of this method dates back to the eighties. It is primarily based on work of Söding (1982), Böttcher (1986) and Pereira (1988, 1989, and 2003). The method simulates large amplitude rigid body motions of mono- and multi hull vessels in six degrees of freedom. Shear forces and bending moments are also determined. In determining the external forces, several assumptions and simplifications were made. These forces comprise:

- forces and moments due to weight,
- Froude-Krylov wave pressures undisturbed by the ship,
- radiation and diffraction pressure, i.e. forces due to the influence of the ship on the pressure field,
- speed effects (resistance and manoeuvring forces),
- propeller and rudder forces (including a proportional-integral-differential -PID-heading controller or a track-keeping controller),
- forces due to fins and bilge keel actions,
- wind forces,
- as well as forces due to fluid motion in tanks and damaged compartments.

Due to the nonlinearity of large ship motions, radiation and diffraction forces cannot be calculated separately. Radiation forces are generated by the ship motions. Radiation forces represent the difference between the forces of the non-moving ship in waves and the Froude-Krylov forces (undisturbed wave forces). If the ship partly emerges from the water, the diffraction component of the emerged part must be zero. Therefore, radiation and diffraction forces are determined using the relative-motion hypothesis. The force is assumed to depend on the motion of the ship minus the motion of the water at the different cross-sections. The orbital velocity of the wave components of the seaway is averaged over a ship cross section. The total force is obtained by integrating the contribution of the ship sections. Longitudinal interactions due to forward speed effects are treated in the same way as for linear strip methods. The pressure distribution not only depends on the instantaneous acceleration of the ship, but also on the preceding accelerations (memory effects). For linear computations in regular waves, these memory effects result in the frequency dependence of the complex added mass matrix, which contains the proportionality constant between the relative motion acceleration of a ship section and the force per length:

$$f = A\ddot{u} \qquad (5)$$

where f and u are 3-component column vectors, while A is a complex 3 by 3 matrix.

For simulations of motions in a natural seaway, the frequency dependency of these

matrices constitutes a challenge, because many frequencies occur at the same time. A solution to this problem is the use of convolution integrals (impulse-response functions), which account for the dependency of these forces on the accelerations at different time steps. The state space model is a faster solution. It uses a relation between acceleration and force derivatives:

$$A_0 \ddot{u} + A_1 \frac{\partial}{\partial t} \ddot{u} + A_2 \frac{\partial^2}{\partial t^2} \ddot{u} \ldots = B_0 + B_1 \dot{f} + B_2 \ddot{f} + \ldots \quad (6)$$

The 3 × 3 matrices A_k and B_k are frequency independent but depend on the actual submergence and roll motion. Implicitly, they are time dependent and are computed from the frequency dependent coefficients by regression analysis. During the simulation, the actual waterline inclination and immersion are considered on the interpolation of the matrices.

4. ROLL DAMPING

The damping moment model comprises a linear and a quadratic term:

$$d_D = -b_L \dot{\varphi} - b_Q \dot{\varphi} |\dot{\varphi}| . \quad (7)$$

The coefficient b_L contains a small speed independent part caused by wave generation of the rolling ship and another (in most cases larger) part that is proportional to the forward speed of the ship and is caused by lift forces generated by hull, propeller, and rudder. The coefficients are taken from Blume (1979). The coefficient b_Q includes bilge keel effects. Blume presents his model test results in diagrams for different breadth/depth ratios and different block coefficients. In his plots, the non-dimensional roll damping coefficient ϕ_{Stat}/ϕ_{Res} is used, which denotes the ratio between the heel angle due to a static moment and the roll amplitude for the equivalent

resonant roll moment. The ratio is dependent on Froude number. To check the accuracy of Blume's coefficients for a modern containership, model tests were carried out. The linear damping constant b_L was determined from forced roll motion model tests (motion excited by rotating masses), using the following equation:

$$b_L = \frac{m \, g \, GM_0}{\omega_r} \left(\frac{\phi_{Stat}}{\phi_{Res}} \right)_{5°} , \quad (7)$$

where ω_r is the roll resonance frequency and GM_0 is the metacentric height.

The nonlinear roll damping coefficient b_Q was also determined from forced roll motion tests. For the resonance angle $\phi_{Res} = 20°$ an effective linear roll damping coefficient b_{eff} was calculated:

$$b_{eff} = \frac{mgGM_0}{\omega_r} \left(\frac{\phi_{Stat}}{\phi_{Res}} \right)_{20°} . \quad (7)$$

For a roll oscillation with frequency ω_r and amplitude $\varphi_A = 20°$, it was assumed that the linear roll damping coefficient b_{eff} is equivalent to the quadratic damping constant b_Q (without bilge keels). To estimate b_Q, the linear component b_L was subtracted from b_{eff}:

$$b_Q = \frac{3\pi}{8 \, \omega_0 \, \varphi_A} (b_{eff} - b_L) \quad (7)$$

The results are shown in Figure 2 and compared with Blume's coefficients derived from experiments carried out in the seventies. The figure clearly shows that the results for zero speed are reasonable, but deviate significantly for higher Froude numbers. For the highest Froude numbers, twice the values compared to Blume's were determined. In all

subsequent calculations, the coefficients derived from our experiments were used.

Roll damping coefficients could have been obtained also on the basis of other approaches, such as on the well-known concept documented by Ikeda et al. (1978). Their approach comprises friction damping, eddy damping, lift damping, and wave damping of the bare hull and normal force damping, hull pressure damping, and wave damping of bilge keels. As we had available experimental data obtained from model test measurements that already accounted for all hull damping components, we used these data to determine damping coefficients for the bare hull. To account for bilge keel damping, we added an equivalent bilge keel damping moment according to Gadd (1964).

5. PREPARATIVE CALCULATIONS

A large number of simulations in regular waves were carried out prior to the model tests to determine which situations regarding wave length and ship speed are relevant for validation purposes. The selected hull form from DSME is shown in Figure 1. The main particulars and investigated load cases of the ship were:

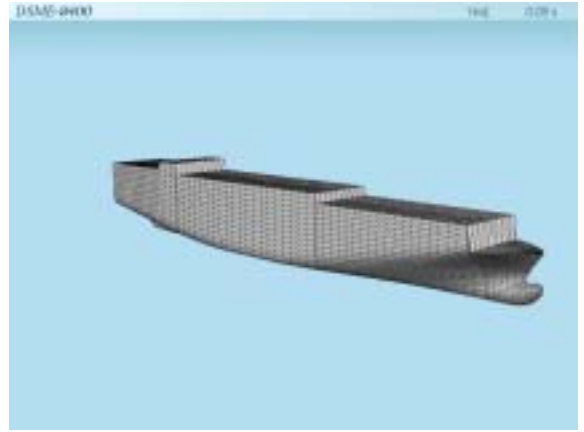| Length over all	332 [m]	
Length b. perp.	317 [m]	
Breadth	43.2 [m]	
Design draught	14.4 [m]	
rxx / B	0.384 [-]	
ryy / Lpp	0.255 [-]	
rzz / Lpp	0.254 [-]	
Load case 1		
GM0		1.26 [m]
Mass		140283
Draught aft		14.647
Draught fore		14.238
Load case 2		
GM0		3.8 [m]
Mass		122908
Draught aft		12.949
Draught fore		12.728

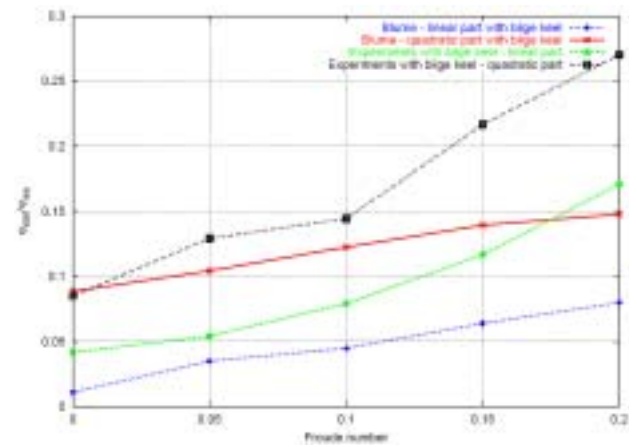Figure 1: Containership Hull Form

Figure 2: Comparison of the non-dimensional roll damping coefficient ϕ_{Stat}/ϕ_{Res} acc. to Blume with model tests

The first load case was chosen as the one with the smallest realistic GM_0 in the stability booklet. Load case 2 was chosen to represent the upper range of realistic transverse stability values. The purpose of this load case was to show the effect of a larger GM_0 on the frequency ratios and the maximum roll angles in parametric roll situations.

The range of wave lengths was set from 70 to 650 m, and Froude numbers from zero speed to $Fn=0.25$ were investigated for wave heights ranging from 2 to 10 m. ROLLSS calculations were performed for 59 wave lengths, 26 speeds, and 5 wave heights. To reduce the computational effort, the number of wave lengths was decreased to 16 for the GL SIMBEL calculations.
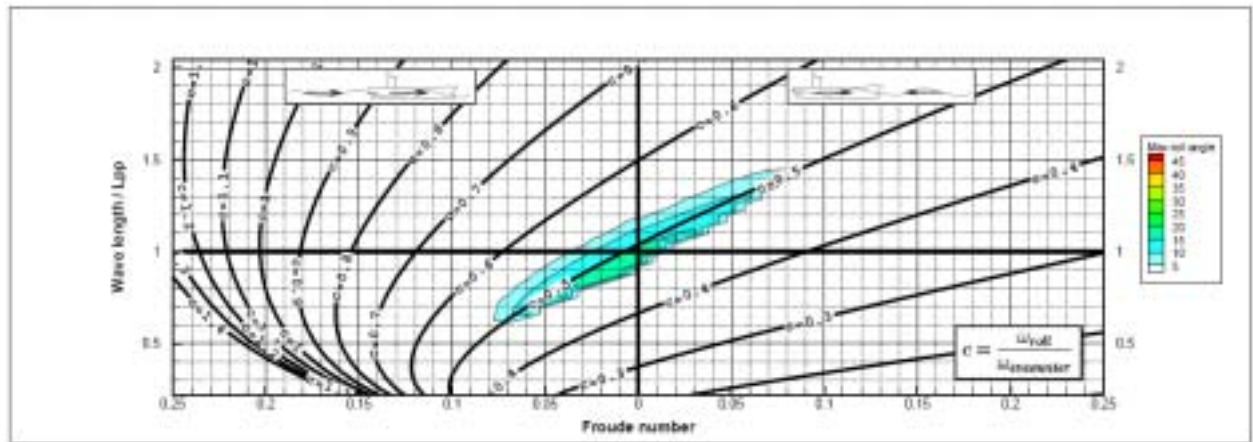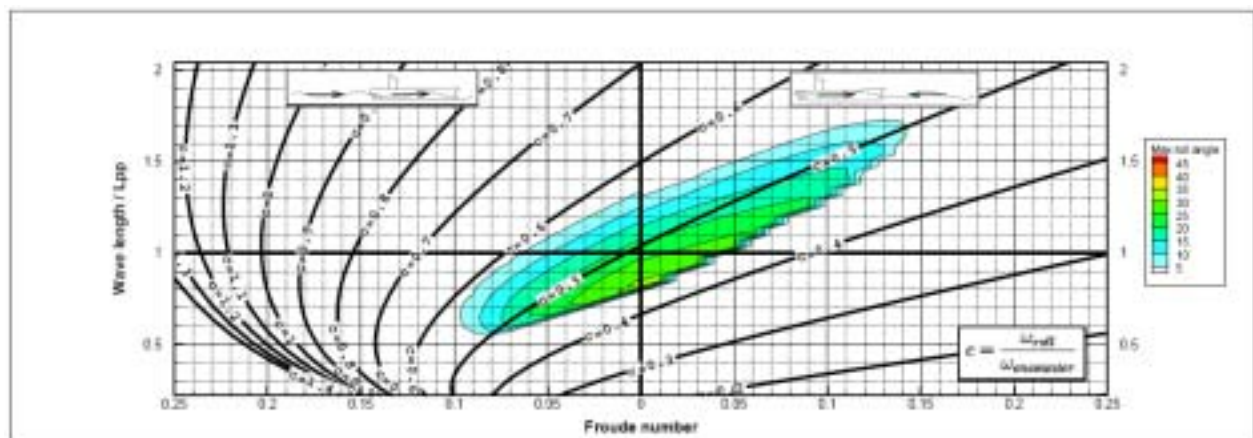
Figure 3: ROLLSS Results for Wave Height 2m

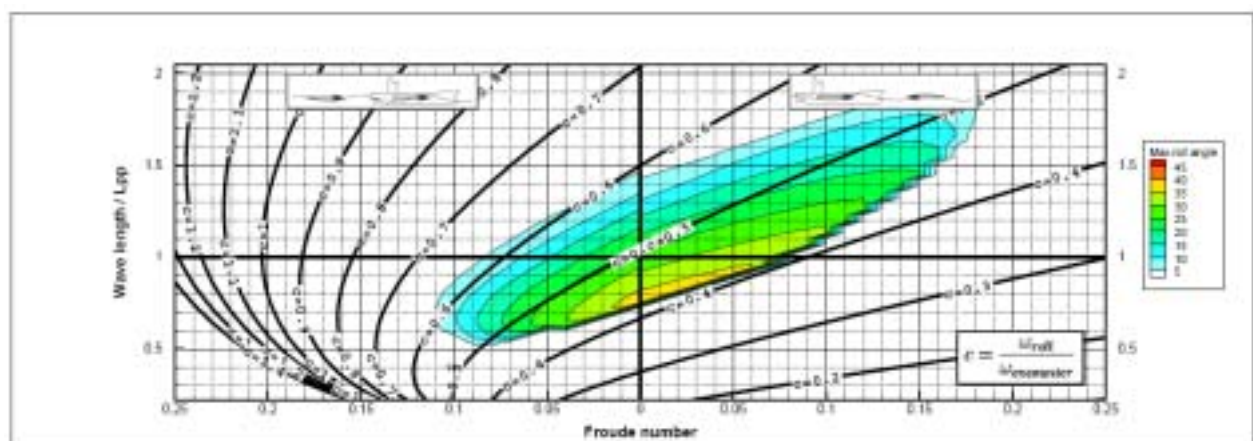Figure 4: ROLLSS Results for Wave Height 4m
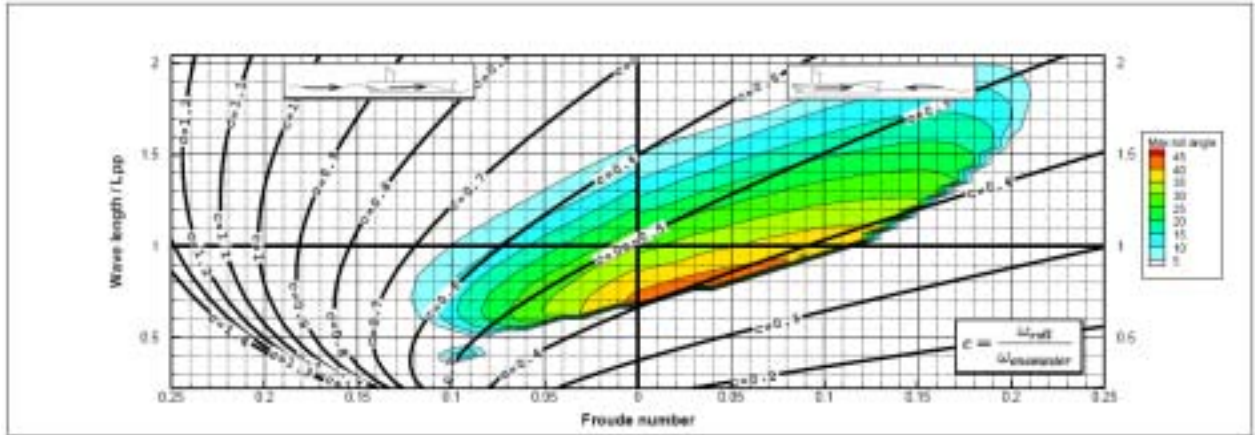
Figure 5: ROLLSS Results for Wave Height 6m

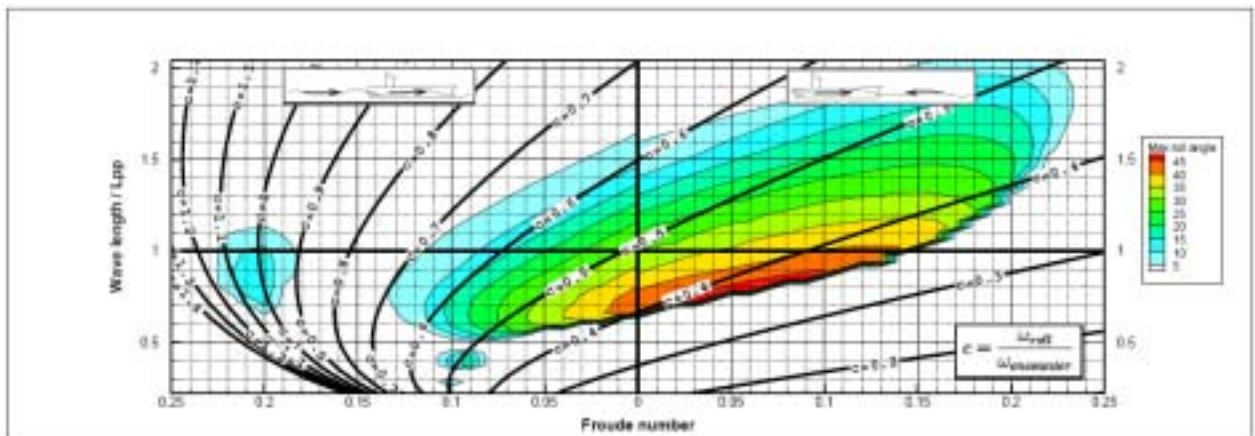Figure 6: ROLLSS Results for Wave Height 8m
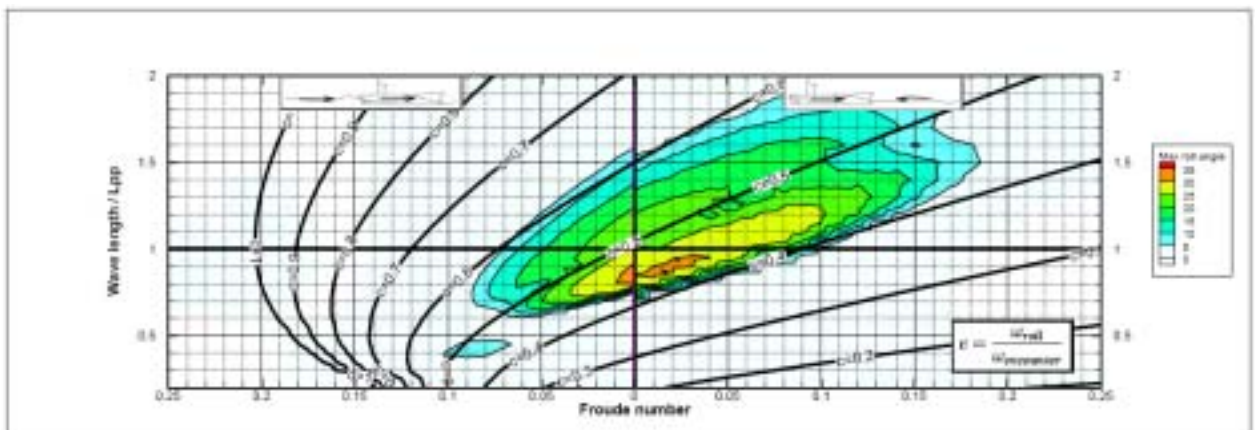

Figure 7: ROLLSS Results for Wave Height 10m

Figure 8: GL SIMBEL Results for Wave Height 8m

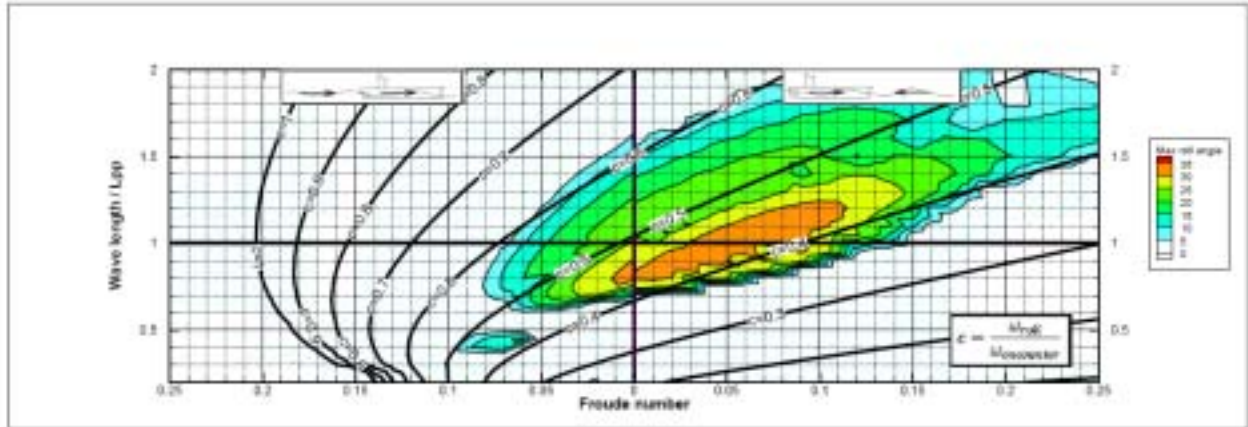Figure 9: GL SIMBEL Results for Wave Height 10m

Table 1: Comparison of Maximum Roll Angles for Head Waves (Wave Height 10m)

Test Run No.	μ [°]	λ/L_{pp}	Fn [-]	φ_{max} [°]		
				Experiments	GL SIMBEL	ROLLSS
10	178	0.6	0.059	0.0	0.1	0.0
18	178	1.0	0.040	30.0	32.1	31.0
19	178	0.9	0.022	31.0	33.3	32.0
21 b	175	0.9	0.065	36.0	37.2	38.0
22	175	0.9	0.030	37.0	32.2	33.0
23	177	1.1	0.052	29.0	31.9	28.0
24	177	1.3	0.076	22.0	28.6	24.0
26	177	1.5	0.068	18.0	21.8	17.0
27	177	1.7	0.061	17.0	15.0	7.5
28	177	2.0	0.085	0.3	0.9	0.0
31	177	1.0	0.052	31.0	33.6	32.0
32	177	1.0	0.108	1.4	37.7	39.0
33 a	177	1.0	0.055	31.0	34.0	32.0
33 b	177	1.0	0.131	22.0	33.2	41.0
34 a	177	1.0	0.099	26.0	38.4	38.0
34 b	177	1.0	0.146	0.0	0.0	0.0

Table 2: Comparison of Maximum Roll Angles for Following Waves (Wave Height 10m)

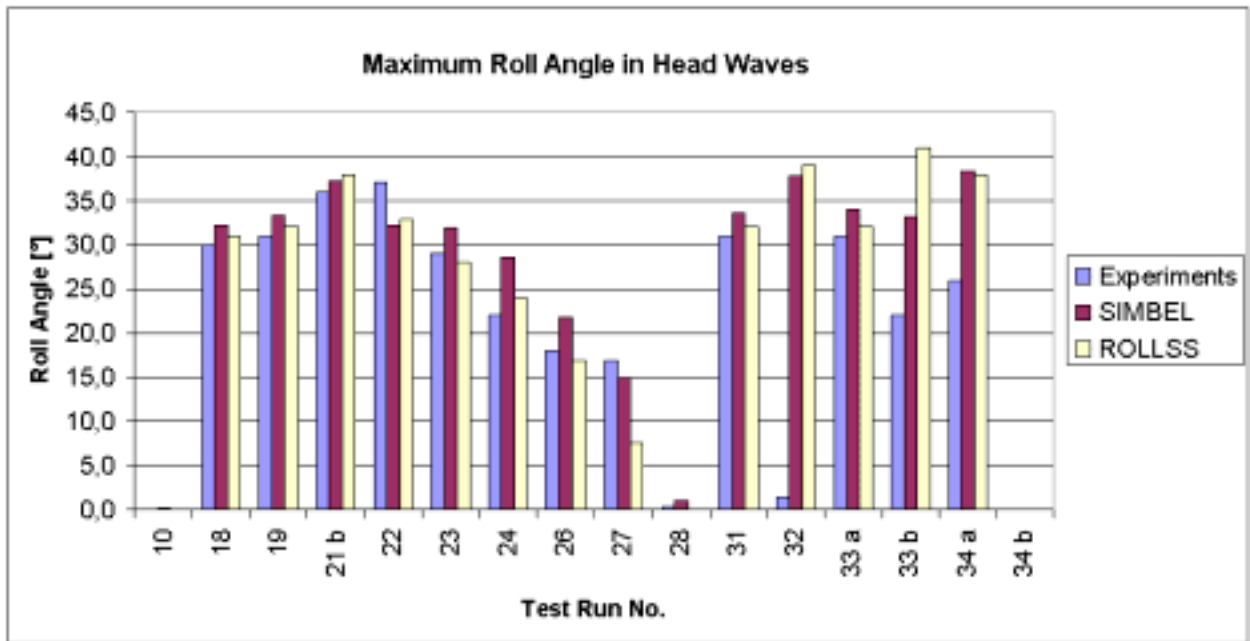| Test Run No.	μ [°]	λ/L_{pp}	Fn [-]	φ_{max} [°]		
				Experiments	GL SIMBEL	ROLLSS
38	3	0.9	0.197	2.5	0.0	15.0
39	3	0.9	0.204	4.0	0.2	15.0
40	5	0.9	0.204	10.0	0.2	16.0
52	5	0.9	0.206	15.0	0.2	16.0
54	2	0.7	0.095	0.7	0.1	15.0
55	2	0.8	0.063	18.5	15.2	22.0
56	0	0.8	0.063	18.0	15.2	22.0
57	0	1.0	0.060	17.0	10.7	17.0

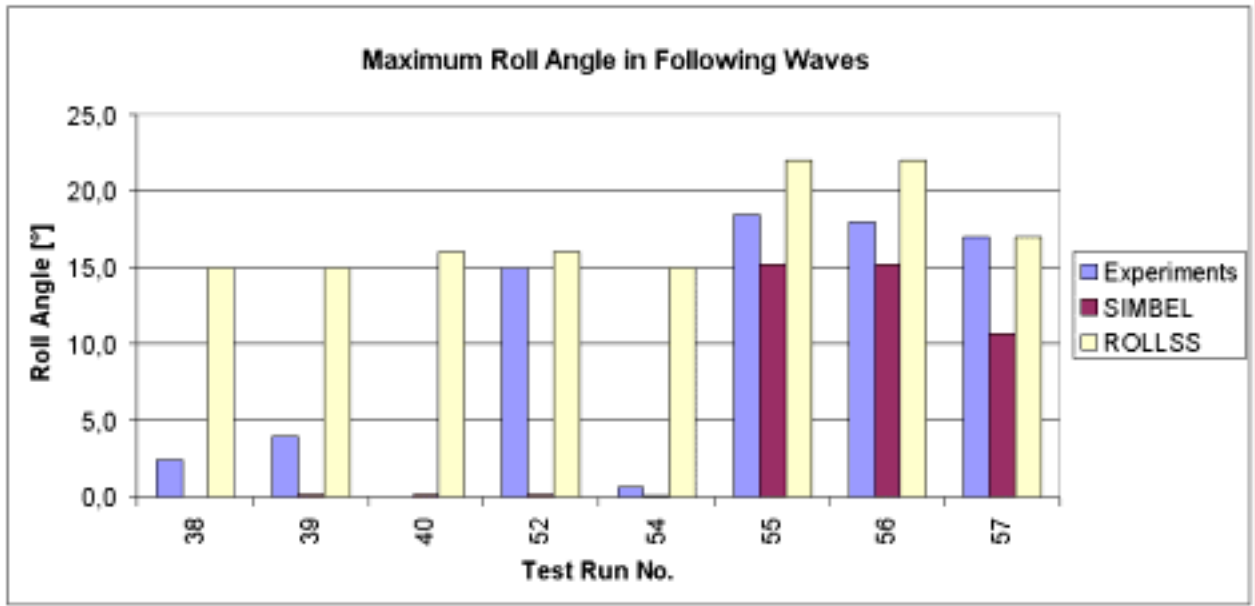Figure 10: Comparison of Simulations and Tests in 10m Head Waves

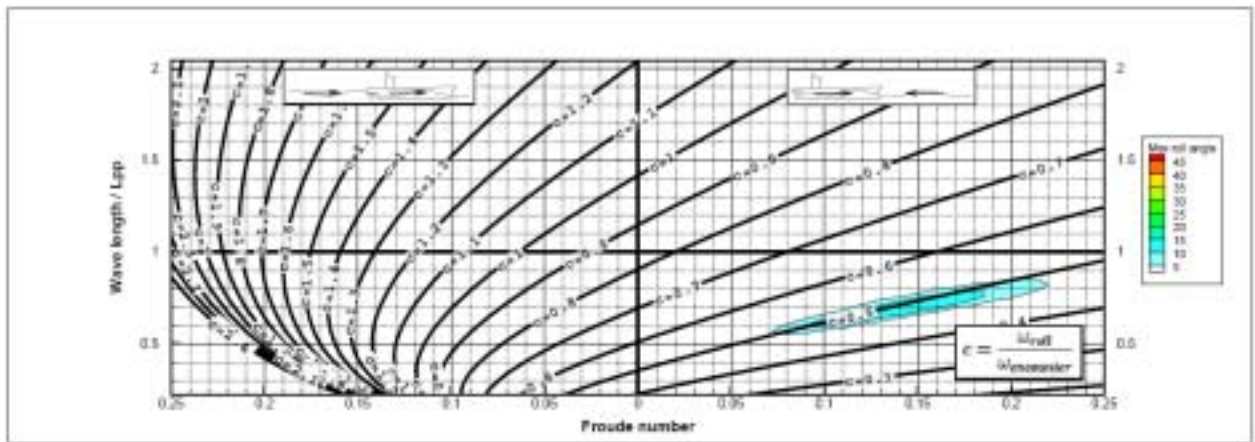Figure 11: Comparison of Simulations and Tests in 10m Following Waves

Figure 12: ROLLSS results for GM_0=3.8m, Wave Height 10m

Figures 3 to 9 show the results for load case 1. The left hand side of the figures depicts the results in following waves, whereas the right hand side shows the results in head waves. ROLLSS and GL SIMBEL yielded similar areas of parametric roll occurrence with small differences in the predicted maximum roll angles. As expected, these areas developed in the vicinity of the frequency ratio 0.5. They become larger for higher wave amplitudes. The boundary towards smaller wavelengths shows a sudden transition from quiescence to large roll amplitudes. The decrease of roll angles towards longer waves is smoother. Only ROLLSS predicted parametric roll with the frequency ratio 1:1 at a wave height of 10 m, see Figure 7.

Figure 12 shows the results for load case 2. The curves of constant frequency ratio are shifted towards lower speeds in following waves and towards higher speeds in head waves. The area of occurrence of parametric roll is narrower than predicted for the smaller GM_0, and maximum roll angles reach only 10° to 15°.

6. MODEL TESTS

In the German research project ROLL-S, a new sophisticated test procedure for a fully automated motion measurement of a free running ship model was developed (Kuehnlein et al. 2003). The ship's course was controlled by the master computer using telemetry. Ship motions in six degrees of freedom were accurately registered by computer controlled guidance of both towing and horizontal carriage. The speed of the propeller had to be fixed before starting the test. This resulted in a strong decrease of the model speed as soon as parametric rolling developed, making it difficult to hold a constant velocity during a test run or to reach a given Froude number.

The model tests were carried out in 10 m high regular waves for load case 1 only. The model scale was 1:53. The angle of encounter was close to 0° (following waves) or 180° (head waves). Because of the limited number of test runs, it was impossible to generate result plots as detailed as for the preparative simulations. Tables 1 and 2 summarise the obtained roll angles of the model tests and the simulations. Figures 10 and 11 show the same data as bar charts.

In following waves for the frequency ratio 1:1, GL SIMBEL simulations did not predict parametric roll for $\lambda/Lpp = 0.9$, compare Fig. 7 and 9. The extensive computer running times of GL SIMBEL set a limit to the number of cases investigated with this method. Consequently, significantly fewer cases were analyzed with GL SIMBEL than with ROLLSS. This situation, in conjunction with

the fact that the mathematical model of these two methods was not identical, possibly brought about the diverse predictions of GL SIMBEL and ROLLSS. Furthermore, for this frequency ratio (test runs no. 38, 39, 40, 52), it was difficult to determine the maximum roll angle in the experiments, because the roll motion still increased when reaching the end of the model basin. Therefore, the test runs for this condition were repeated several times, and the results did not show a clear trend for the maximum roll angles, see Table 2.

7. CONCLUSIONS

A large number of simulations were carried out using GL SIMBEL and ROLLSS. Model tests in regular waves were performed and the results were compared to the simulations. The results of simulations and experiments compared favourably for most test runs. The head sea experiments 32, 33b and 34a for situations close to the steep transition from quiescence to large roll angles showed bad correlation with the simulations.

For the frequency ratio 1:1 in following waves (test runs no. 38, 39, 40, 52) it was difficult to determine the maximum roll angle in the experiments because the roll motion still increased when reaching the end of the model basin.

Both methods demonstrated their ability to predict the occurrence of parametric roll in head and following seas. Although ROLLSS is based on a simpler mathematical model than GL SIMBEL, both methods predicted similar roll. This demonstrated that the chosen approaches were well suited for the phenomena investigated here. The main factor that causes the parametric roll, changes in the wetted surface of the ship, is captured in both methods. ROLLSS takes this into account with pre-calculated heeling arm curves and GL SIMBEL calculates the hydrostatic pressure at the actual position of

the ship at each time instant. For other headings, the accuracy of GL SIMBEL is expected to be better due to the nonlinear coupling of all ship motions. However, this was not yet experimentally validated.

The importance to re-evaluate the roll damping coefficients for modern ship designs was demonstrated. The next phase of DYNAS focuses on the validation of the numerical codes in irregular sea ways.

8. REFERENCES

Blume, P., 1979, "Experimentelle Bestimmung der Koeffizienten der wirksamen Rolldämpfung und ihre Anwendung zur Abschätzung extremer Rollwinkel", Schiffstechnik, Vol. 26.

Böttcher, H., 1986, "Ship motion simulation in a seaway using detailed hydrodynamic force coefficients", STAB 1986, 3rd International Conference on Stability of Ships and Ocean Vehicles, Gdansk.

Gadd, G.E., 1964, "Bilge keels and bilge vanes", Report Nr. 64, National Physical Laboratory , Ship Division .

Hachmann, D., 1991, "Calculation of Pressures on a Ship's Hull in Waves", Ship Technology Research, Vol. 38, No. 3.

Ikeda, Y.; Himeno, Y.; Tanaka, N., 1978, "A Prediction Method for Ship Roll Damping", Department on Naval Architectural, University of Osaka Prefecture, Report Nr. 00405.

Kröger, H.P., 1986, "Rollsimulation von Schiffen im Seegang", Schiffstechnik, Vol. 33.

Kuehnlein, W.L.; Brink, Kay-Enno; Hennig, J., 2003, "Innovative deterministic seakeeping test procedures", STAB 2003, 8th International Conference on the Stability of Ships and Ocean Vehicles, Madrid.

Papanikolaou, A.D.; Schellin, T.E., 1991, "A Three-Dimensional Panel Method for Motions and Loads of Ships with Forward Speed", Ship Technology Research, Vol. 39, No. 4.

Pereira, R, 1988, "Simulation nichtlinearer Seegangslasten", Schiffstechnik, Vol. 35-4, pp. 173-193.

Pereira, R., 1989, "Ermittlung der Belastungen von Schiffen in steilem Seegang durch Simulation", Jahrbuch der Schiffbautechnischen Gesellschaft, Summer Meeting, Berlin, Vol. 83, pp. 145-158.

Pereira, R., 2003, "Numerical Simulation of Capsizing in Severe Seas", STAB 2003, 8th International Conference on the Stability of Ships and Ocean Vehicles, Madrid

Petey, F., 1988, "Ermittlung der Kentersicherheit lecker Schiffe im Seegang aus Bewegungssimulationen", Report Nr. 487, Institut für Schiffbau der Universität Hamburg

SNAME AD HOC PANEL #13, 2003, "Investigation of head-sea parametric rolling and resulting vessel and cargo securing loads", Marine Technology , 41.

Söding, H, 1982, "Leckstabilität im Seegang", Report Nr. 429, Institut für Schiffbau der Universität Hamburg